Variable kinematic models applied to free vibration analysis of functionally graded materials shells.

Variable kinematic models applied to free-vibration analysis of functionally graded material shells

M. Cinefra [a,b], S. Belouettar [b], M. Soave [a], E. Carrera [a,*]

[a] Department of Aeronautics and Space Engineering, Politecnico di Torino, Corso Duca degli Abruzzi, 24, 10129 Torino, Italy
[b] CRP H Tudor, Esch-sur-Alzette, Luxembourg

A B S T R A C T

Closed-form solutions of free-vibration problems of simply supported multilayered shells made of Functionally Graded Material have been examined in the present paper. A variable kinematic shell model, which is based on Carrera's Unified Formulation is extended, in this work, to dynamic shell cases. Classical shell theories are compared to refined ones as well as to layer-wise kinematics and mixed assumptions based on the Reissner mixed variational theorem. A comparison with the few results available in the open literature is presented and conclusions are drawn regarding the accuracy of classical and advanced shell modeling to evaluate lower and higher vibration modes as well as the behavior of these modes in the shell thickness direction.

1. Introduction

Functionally graded materials (FGMs) have been the subject of numerous studies in the recent past. FGMs are classified as a family of composite materials; they are characterized by a functional variation in the composition of the material properties through an assigned direction, which often coincides with the thickness direction. Their particular feature is that they have the characteristic behavior of composite materials, but they do not show material discontinuities at the interfaces of a classical laminate. Their composition, and therefore their manufacturing, are designed to optimize the use of materials, mostly by reducing the weight of the structure. This is obtained by modifying the constituent phases through grading (mathematical) laws. FGMs are able to offer benefits compared to traditional laminates. The constituent phases, which may be more than two, are adjusted by varying the volume fractions whose rates are in turn related to the mathematical law that is used. The benefits associated with the presence of such materials are significant: the possibility of reducing the interlaminar discontinuities which are the main cause of delamination and the consequent failure of classical laminates.

Various FGM power laws have been used in the open literature, some of which have been provided by Mori and Tanaka (1973), Kashtalyan (2004) and Zenkour (2006). Among the various topics related to FGM, reference can be made to the review articles by Birman and Bird (2007). The present work is focused on refined shell models for accurate free-vibration analysis of layered shell with FGM layers. Several works concerning FG shell vibration have been presented over the last year. A short review, that is useful for our purpose, is given below.

Loy et al. (1999) have studied the vibrations of functionally graded cylindrical shells. The results show that the frequency characteristics are similar to those observed for homogeneous isotropic cylindrical shells and that the frequencies are affected by the constituent volume fractions and the configurations of the constituent materials. The analysis was carried out with strain-displacement relations from the Love shell theory and the eigenvalue governing equation was obtained using the Rayleigh–Ritz method. Pradhan et al. (2000) have examined the vibration characteristics of functionally graded cylindrical shells under various boundary conditions. The Rayleigh method was used to derive the governing equations. The effects of boundary conditions and volume fractions (power law exponent) on the natural frequencies were studied; it has been shown that the frequency characteristics of the FG shell are found to be similar to those of isotropic cylindrical shells. Chen et al. (2004) have proposed a three-dimensional vibration analysis of fluid-filled orthotropic FGM cylindrical shells. A state equation, with variable coefficients, was derived in a unified matrix form on the basis of the three-dimensional fundamental equations of anisotropic elasticity. A laminate approximate model,

which is suitable for an arbitrary variation of the material constants along the radial direction was employed; numerical examples are presented and compared with existing results. Tornabene (2009) has conducted a free-vibration analysis of functionally graded conical, cylindrical shell and annular plate structures with proposed a four-parameter power law distribution. Based on the First-order Shear Deformation Theory (FSDT), the discretization of the system equations was made by means of the Generalized Differential Quadrature. Few works are available on the free vibration of FGM shells and none of these quotes the assessment of advanced or classical theories.

The present work deals with variable kinematic models in the framework of Carrera's Unified Formulation (CUF) for the analysis of FGM shells. CUF was originally developed for classical layered structures (Carrera, 1998a, 2003); it has has been extended to FGM structure by Carrera et al. (2008). The generalized expansion, upon which the CUF is based, relies on a set of functions which are indicated as thickness functions. CUF reduces a three-dimensional problem to a bi-dimensional one and the order of expansion along the thickness of the plate is taken as a free parameter of the problem. As a result, an exhaustive variable kinematic model is obtained.

The principle of virtual displacements (PVD) has been employed in Carrera et al. (2008), while Reissner's mixed variational theorem (RMVT) has been extended to FGM in Brischetto and Carrera (in press). RMVT permits one to assume both displacement and transverse shear/normal stress variables. Related plate/shell bending problems have recently been analyzed in Carrera et al. (in press). Application to FGM beams has been given in Giunta et al. (in press) where several refined beam theories were applied to the linear static analysis of beams made of FGM. The extension of CUF to vibration analysis for plates has been discussed in Cinefra and Soave (in press).

In the present work the variable kinematic model is extended to the dynamic analysis of FGM shells, and the natural frequencies of single-layered shells are compared to other available solutions. Both PVD and RMVT are employed to compare classical and mixed shell theories.

The article has been organized as follows: the shell geometry is given in Section 2; the used variational statements and constitutive equations are given in Sections 3 and 3.3, respectively; the considered shell theories are described in Sections 4 and 5; the closed-form solution for the considered free-vibration problem is described in Section 6; the numerical discussion is conducted in Section 7.

2. Geometry

Shells are two-dimensional structures with one dimension, in general the thickness in the z direction, negligible with respect to the other two in the plane directions. The shells present radii of curvature R_α and R_β along the two in-plane directions α and β, respectively. A curvilinear reference system (α, β, z) for shells is indicated in Fig. 1. In the case of layered shells, the reference surface of the k-layer is denoted by Ω_k, and the curvilinear coordinates are α_k and β_k. The following differential relation holds (Kraus, 1967):

$$\begin{aligned} \mathrm{d}s_k^2 &= H_\alpha^k \mathrm{d}\alpha_k^2 + H_\beta^k \mathrm{d}\beta_k^2 + H_z^k \mathrm{d}z_k^2 \\ \mathrm{d}\Omega_k &= H_\alpha^k H_\beta^k \mathrm{d}\alpha_k \mathrm{d}\beta_k \\ \mathrm{d}V &= H_\alpha^k H_\beta^k H_z^k \mathrm{d}\alpha_k \mathrm{d}\beta_k \mathrm{d}z_k \end{aligned} \tag{1}$$

In the case of shells with constant radii of curvature, the geometrical relations are written in the following matrix form:

$$\boldsymbol{\epsilon}_{pG}^k = \left[\epsilon_{\alpha\alpha}^k, \epsilon_{\beta\beta}^k, \gamma_{\alpha\beta}^k\right]^T = (\boldsymbol{D}_p^k + \boldsymbol{A}_p^k)\boldsymbol{u}^k, \tag{2}$$

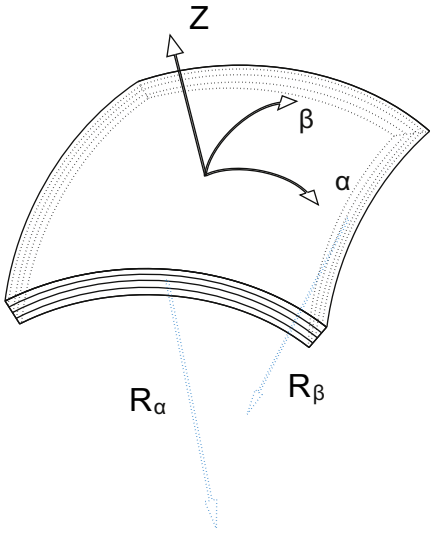

Fig. 1. Geometry and reference system for multilayered shells.

$$\boldsymbol{\epsilon}_{nG}^k = \left[\gamma_{\alpha z}^k, \gamma_{\beta z}^k, \epsilon_{zz}^k\right]^T = (\boldsymbol{D}_{np}^k + \boldsymbol{D}_{nz}^k - \boldsymbol{A}_n^k)\boldsymbol{u}^k, \tag{3}$$

where for each layer k the vector of displacement components is $\boldsymbol{u}^k = (u^k, v^k, w^k)$. The explicit form of the introduced arrays follows:

$$\boldsymbol{D}_p^k = \begin{bmatrix} \frac{\partial_\alpha}{H_\alpha^k} & 0 & 0 \\ 0 & \frac{\partial_\beta}{H_\beta^k} & 0 \\ \frac{\partial_\beta}{H_\beta^k} & \frac{\partial_\alpha}{H_\alpha^k} & 0 \end{bmatrix}, \quad \boldsymbol{D}_{np}^k = \begin{bmatrix} 0 & 0 & \frac{\partial_\alpha}{H_\alpha^k} \\ 0 & 0 & \frac{\partial_\beta}{H_\beta^k} \\ 0 & 0 & 0 \end{bmatrix},$$

$$\boldsymbol{D}_{nz}^k = \begin{bmatrix} \partial_z & 0 & 0 \\ 0 & \partial_z & 0 \\ 0 & 0 & \partial_z \end{bmatrix}. \tag{4}$$

$$\boldsymbol{A}_p^k = \begin{bmatrix} 0 & 0 & \frac{1}{H_\alpha^k R_\alpha^k} \\ 0 & 0 & \frac{1}{H_\beta^k R_\beta^k} \\ 0 & 0 & 0 \end{bmatrix}, \quad \boldsymbol{A}_n^k = \begin{bmatrix} \frac{1}{H_\alpha^k R_\alpha^k} & 0 & 0 \\ 0 & \frac{1}{H_\beta^k R_\beta^k} & 0 \\ 0 & 0 & 0 \end{bmatrix}. \tag{5}$$

The coefficients H^k are:

$$H_\alpha^k = A^k\left(1 + \frac{z_k}{R_\alpha^k}\right), H_\alpha^k = B^k\left(1 + \frac{z_k}{R_\beta^k}\right), H_z^k = 1$$

where A^k and B^k are the coefficients of first fundamental form of reference surface and them, for shells to have constant curvature, have unit value. ($A^k = B^k = 1$).

3. Variational statements

3.1. Principle of Virtual Displacement − PVD

Classical displacements formulations consider displacements $\mathbf{u}$ as primary variables. The following two-dimensional approximation is introduced in a very general form:

$$\boldsymbol{u} = F_\tau \boldsymbol{u}_\tau, \quad \tau = 1, \ldots, N \tag{6}$$

where

$$\boldsymbol{u} = \left(u_\alpha, u_\beta, u_z\right) \quad \text{and} \quad \boldsymbol{u}_\tau = \left(u_{\alpha\tau}, u_{\beta\tau}, u_{z\tau}\right) \tag{7}$$

$\boldsymbol{u}$ are displacements in each point $P(\alpha, \beta, z)$, $\boldsymbol{u}_\tau$ are displacements in each point $P_\Omega(\alpha, \beta)$ on the reference surface Ω. F_τ are the introduced thickness functions.

The Principle of Virtual Displacements (PVD) states (Washizu, 1968):

$$\int_V (\delta\boldsymbol{\epsilon}_{pG}^T\boldsymbol{\sigma}_{pC} + \delta\boldsymbol{\epsilon}_{nG}^T\boldsymbol{\sigma}_{nC})\mathrm{d}V = \int_V \rho\delta\mathbf{u}\ddot{\mathbf{u}}\mathrm{d}V + \delta L_e, \tag{8}$$

where T indicates the transpose of considered array and V is the volume of body; ρ indicates the mass density. The subscript p indicates the in-plane component of strains and deformations, $\sigma_p = [\sigma_{\alpha\alpha}, \sigma_{\beta\beta}, \sigma_{\alpha\beta}]$, and $\epsilon_p = [\epsilon_{\alpha\alpha}, \epsilon_{\beta\beta}, \gamma_{\alpha\beta}]$. The subscript n indicates the out-of-plane components, $\sigma_n = [\sigma_{\alpha z}, \sigma_{\beta z}, \sigma_{zz}]$, and $\epsilon_n = [\gamma_{\alpha z}, \gamma_{\beta z}, \epsilon_{zz}]$. δL_e is the external virtual work. $\ddot{\mathbf{u}}$ indicates the second derivative of displacements with respect to time. Subscript C and G indicate the use of constitutive equations and geometrical relations, respectively.

3.2. Reissner Mixed Variational Theorem − RMVT

In order to fulfill 'a priori' interlaminar continuity of transverse shear and normal stress component in laminated structures, Reissner (1984) introduced Reissner Mixed Variational Theorem (RMVT) (Carrera, 2001):

$$\mathbf{u} = F_\tau\mathbf{u}_\tau, \boldsymbol{\sigma}_{n\mathrm{M}} = F_\tau\boldsymbol{\sigma}_{n\mathrm{M}\tau}, \tag{9}$$

The subscript M indicates assumed (modeled) values: $\sigma_{nM\tau} = [\sigma_{\alpha z}, \sigma_{\beta z}, \sigma_{zz}]$. RMVT states:

$$\int_V (\delta\boldsymbol{\epsilon}_{pG}^T\boldsymbol{\sigma}_{pC} + \delta\boldsymbol{\epsilon}_{nG}^T\boldsymbol{\sigma}_{n\mathrm{M}} + \delta\boldsymbol{\sigma}_{n\mathrm{M}}^T(\boldsymbol{\epsilon}_{nG} - \boldsymbol{\epsilon}_{nC}))\mathrm{d}V) = \int_V \rho\delta\mathbf{u}\ddot{\mathbf{u}}\mathrm{d}V + \delta L_e. \tag{10}$$

3.3. Hooke Law for PVD and RMVT

Classical Hooke law for a layer k embedded in a multilayered structure is:

$$\boldsymbol{\sigma}_{pC}^k = \mathbf{Q}_{pp}^k(z)\boldsymbol{\epsilon}_{pG}^k + \mathbf{Q}_{pn}^k(z)\boldsymbol{\epsilon}_{nG}^k, \tag{11}$$

$$\boldsymbol{\sigma}_{nC}^k = \mathbf{Q}_{np}^k(z)\boldsymbol{\epsilon}_{pG}^k + \mathbf{Q}_{nn}^k(z)\boldsymbol{\epsilon}_{nG}^k. \tag{12}$$

where Q_{pp}^k, Q_{pn}^k, Q_{np}^k, Q_{nn}^k are $[3 \times 3]$ sub-arrays containing the elastic coefficients for an orthotropic layer in the structure reference system (see Carrera, 1995).

In case of RMVT applications, Hooke law is rewritten in the following mixed form:

$$\boldsymbol{\sigma}_{pC}^k = \widehat{\mathbf{Q}}_{pp}^k(z)\boldsymbol{\epsilon}_{pG}^k + \widehat{\mathbf{Q}}_{pn}^k(z)\boldsymbol{\sigma}_{n\mathrm{M}}^k, \tag{13}$$

$$\boldsymbol{\epsilon}_{nC}^k = \widehat{\mathbf{Q}}_{np}^k(z)\boldsymbol{\epsilon}_{pG}^k + \widehat{\mathbf{Q}}_{nn}^k(z)\boldsymbol{\sigma}_{n\mathrm{M}}^k, \tag{14}$$

where the new coefficients are:

$$\begin{aligned}
\widehat{\mathbf{Q}}_{pp}^k(z) &= \mathbf{Q}_{pp}^k(z) - \mathbf{Q}_{pn}^k(z)\mathbf{Q}_{nn}^k(z)^{-1}\mathbf{Q}_{np}^k(z),\\
\widehat{\mathbf{Q}}_{pn}^k(z) &= \mathbf{Q}_{pn}^k(z)\mathbf{Q}_{nn}^k(z)^{-1},\\
\widehat{\mathbf{Q}}_{np}^k(z) &= -\mathbf{Q}_{nn}^k(z)^{-1}\mathbf{Q}_{np}(z), \quad \widehat{\mathbf{Q}}_{nn}^k(z) = \mathbf{Q}_{nn}^k(z)^{-1}.
\end{aligned} \tag{15}$$

In case of FGM layers, the coefficients in Eqs. (11), (15), and (13) vary in the thickness direction z according to a given law:

$$\mathbf{Q}(z) = \mathbf{Q}_0 \times g(z), \tag{16}$$

where $\mathbf{C}_0$ is the reference stiffness matrix and $g(z)$ gives the variation along z. For convenience, the thickness functions given in Eq. (3), are used to approximate $Q(z)$:

$$\mathbf{Q}(z) = F_b(z)\mathbf{Q}_b + F_t(z)\mathbf{Q}_t + F_\gamma(z)\mathbf{Q}_\gamma = F_r\mathbf{Q}_r \text{ with } r = 1, \ldots, 10 \tag{17}$$

where $\mathbf{Q}_r$ are constant in z and *thickness functions* F_r are a combination of Legendre polynomials. Previous formula consists of the unique novelty for the introduction of FGM in the variable kinematic model in the CUF. By considering the approximation given in Eq. (17), it is possible to obtain a general form of constitutive relations for the PVD and RMVT case, they are valid for both cases of functionally graded materials and materials with constant properties through the thickness direction z. For the PVD models, the constitutive equations are:

$$\boldsymbol{\sigma}_{pC}^k = F_r\mathbf{Q}_{ppr}^k\boldsymbol{\epsilon}_{pG}^k + F_r\mathbf{Q}_{pnr}^k\boldsymbol{\epsilon}_{nG}^k, \tag{18}$$

$$\boldsymbol{\sigma}_{nC}^k = F_r\mathbf{Q}_{npr}^k\boldsymbol{\epsilon}_{pG}^k + F_r\mathbf{Q}_{nnr}^k\boldsymbol{\epsilon}_{nG}^k. \tag{19}$$

In the case of RMVT models, the constitutive equations state:

$$\boldsymbol{\sigma}_{pC}^k = F_r\widehat{\mathbf{Q}}_{ppr}^k\boldsymbol{\epsilon}_{pG}^k + F_r\widehat{\mathbf{Q}}_{pnr}^k\boldsymbol{\sigma}_{nM}^k, \tag{20}$$

$$\boldsymbol{\epsilon}_{nC}^k = F_r\widehat{\mathbf{Q}}_{npr}^k\boldsymbol{\epsilon}_{pG}^k + F_r\widehat{\mathbf{Q}}_{nnr}^k\boldsymbol{\sigma}_{n\mathrm{M}}^k, \tag{21}$$

where $k = 1, \ldots, N_l$ indicates the considered layers, and $r = 1, \ldots, 10$ is the loop to approximate the FGM properties varying with the z coordinate. In the case of materials with constant properties in z, the loop on r index is not necessary and the material coefficients are constant.

4. Considered shell theories

CUF permits to introduce several two-dimensional models for shells. The governing equations are written, in a unified form, in terms of few *fundamental nuclei* which form do not formally depend on the order of expansion N that is used in the z direction as well as on the variables description used in the multilayered structure (Layer-Wise (LW) or Equivalent Single Layer (ESL)).

The generic variable $\mathbf{a}(\alpha, \beta, z)$ and its variation $\delta\mathbf{a}(\alpha, \beta, z)$ can be written according to the following general expansions:

$$\mathbf{a}(\alpha,\beta,z) = F_\tau(z)\mathbf{a}_\tau(\alpha,\beta), \delta\mathbf{a}(\alpha,\beta,z) = F_s(z)\delta\mathbf{a}_s(\alpha,\beta) \text{ with } \tau, s = 1, \ldots, N \tag{22}$$

Bold letters denote arrays; the summing convention with repeated indexes τ and s is assumed. Depending on the used thickness functions, a model can be: ESL when the variable is assumed for the whole multilayer or LW when the variable is considered independent in each layer. Any shell configuration embedding FGM layers can be considered: a single-layer FGM shell or a multilayered structure with a functionally graded core. The proposed two-dimensional models have been coded according to the CUF. Details can be found in previous authors' works (Carrera et al., 2008; Carrera, 1995, 2002).

4.1. Equivalent single-layer theories

Higher Order Theories (HOTs) for displacement variables $\mathbf{u}$ can be formulated according to the following expansion:

$$u_\tau(\alpha,\beta,z) = u_{0\tau}(\alpha,\beta) + z^i \quad u_{i\tau}(\alpha,\beta) \quad \text{with} \quad \tau = \alpha,\beta \quad \text{and} \quad i = 1, N. \tag{23}$$

where u_0 denotes the displacements value in correspondence to the reference surface Ω and u_i is the i-th derivative of u. The summing

convention for the repeated indexes has been adopted. N is the order of expansion, which is taken as a free parameter. In the numerical investigation N is considered to range from 1 to 4.

According to the acronym system developed within CUF, the related theories are named as $ED1-ED4$. The letter E denotes that the kinematic is preserved for the whole layers, as in the ESL approach. D denotes that only displacement unknowns are used and the last number states the through-the-thickness expansion order. Classical Lamination Theory (CLT), based on Cauchy (1828), Poisson (1829) or Kirchhoff (1850) assumptions type, discards transverse shear and through-the-thickness deformations. The displacement model related to CLT can be written in the following form:

$$\begin{aligned} u_\tau(\alpha,\beta,z) &= u_{0\tau}(\alpha,\beta) - z\frac{\partial u_{0z}(\alpha,\beta)}{\partial\tau} \quad \text{with} \quad \tau = \alpha,\beta \\ u_z(\alpha,\beta,z) &= u_{0z}(\alpha,\beta). \end{aligned} \tag{24}$$

It states that the section remains plane and orthogonal to the plate reference surface Ω. Transverse shear/normal stresses are discarded by CLT.

Transverse shear deformations can be introduced according to Reissner and Mindlin's (see Reissner, 1945 and Mindlin, 1951) kinematic assumptions:

$$\begin{aligned} u_\tau(\alpha,\beta,z) &= u_{0\tau}(\alpha,\beta) + z \quad u_{1\tau}(\alpha,\beta) \quad \text{with} \quad \tau = \alpha,\beta \\ u_z(\alpha,\beta,z) &= u_{0z}(\alpha,\beta). \end{aligned} \tag{25}$$

This theory is also denoted as First-order Shear Deformation Theory (FSDT) in case of laminated structures. Transverse shear stresses show "a priori" constant piece-wise distribution.

FSDT can be obtained from $ED1$ theory considering a constant transverse displacement through the thickness. In both CLT and FSDT, Poisson locking phenomena is contrasted by means of the plane-stress conditions as indicated in Carrera and Brischetto (2008a,b). That correction is also used in the $ED1$ cases.

4.2. Layer-Wise Theories

Multilayered shells can be analyzed by kinematics assumptions which are independent in each layer k. According to Reddy (2004) these approaches are herein stated as Layer-Wise theories.

LW description yields, thus, displacement variables that are independent in each layer. The Taylor thickness expansion, adopted in the previous paragraphs for ESL cases, is not convenient for LW description. Displacements interlaminar continuity can be imposed more conveniently by employing interface values as unknown variables. LW description assumes the following form:

$$\begin{aligned} u_\tau^k &= F_t u_{\tau t}^k + F_b u_{\tau b}^k + F_r u_{\tau r}^k \quad \text{with} \\ \tau &= \alpha,\beta,z,r = 2,3,\ldots,N, k = 1,2,\ldots,N_l. \end{aligned} \tag{26}$$

where N_l indicates the number of layers. Subscripts t and b denote values related to the top and the bottom of layer, respectively. The thickness functions $F_\tau(\zeta_k)$ have been defined by:

$$F_t = \frac{P_0+P_1}{2}, \quad F_b = \frac{P_0-P_1}{2}, \quad F_r = P_r - P_{r-2}, \quad r = 2,3,\ldots,N, \tag{27}$$

in which $P_j = P_j(\zeta_k)$ is the Legendre's j^{th}-order polynomial defined in the ζ_k-domain: $-1 \le \zeta_k \le 1$. In the numerical investigations the maximum order is considered to be four, related polynomials are:

$$P_0 = 1, \quad P_1 = \zeta_k, \quad P_2 = \left(3\zeta_k^2 - 1\right)\Big/2,$$
$$P_3 = \frac{5\zeta_k^3}{2} - \frac{3\zeta_k}{2}, \quad P_4 = \frac{35\zeta_k^4}{8} - \frac{15\zeta_k^2}{4} + \frac{3}{8}.$$

The previous functions have the following interesting properties:

$$\zeta_k = \begin{cases} 1 : F_t = 1; & F_b = 0; \quad F_r = 0 \\ -1 : F_t = 0; & F_b = 1; \quad F_r = 0. \end{cases} \tag{28}$$

The top and bottom values have been used as unknown variables. The interlaminar compatibility of displacement can be therefore easily linked:

$$u_{\tau t}^k = u_{\tau b}^{(k+1)}, \quad k = 1, \ N_l - 1. \tag{29}$$

The acronyms for these theories are $LD1-LD4$ where L means LW approach. LW mixed models based on RMVT consider the letter M instead of D. Related layer-wise analysis are denoted as $LM1-LM4$.

5. Governing equations

This section presents the dynamic governing equations based on the variational statements of Section 2. The derivation of governing equation permits to obtain the so-called *fundamental nuclei*. These

Table 1
Comparison of frequency parameter $\overline{\omega} = \omega h\sqrt{\rho_c/E_c}$ vs thickness ratio h/R, vibration modes m and exponent p. Shell data: $b/R = 2$, FGM Al/Al_2O_3.

h/R	m	Ref. Matsunaga (2009)	$LM4$	$ED4$	CLT	FSDT
$p = 1$						
0.500	2	0.2720E0	0.2765E0	0.2768E0	0.2725E0	0.2725E0
0.200	4	0.7218E−1	0.7117E−1	0.7113E−1	0.7206E−1	0.7137E−1
0.100	6	0.2821E−1	0.2771E−1	0.2766E−1	0.2792E−1	0.2770E−1
0.050	6	0.1020E−1	0.1013E−1	0.1013E−1	0.1015E−1	0.1014E−1
0.010	10	0.9454E−3	0.9446E−3	0.9434E−3	0.9438E−3	0.9436E−3
0.001	18	0.3068E−4	0.3090E−4	0.3090E−4	0.3090E−4	0.3090E−4
$p = 4$						
0.500	2	0.2209E0	0.2258E0	0.2261E0	0.2233E0	0.2233E0
0.200	4	0.5995E−1	0.5884E−1	0.5879E−1	0.5980E−1	0.5912E−1
0.100	6	0.2391E−1	0.2334E−1	0.2330E−1	0.2359E−1	0.2336E−1
0.050	6	0.8449E−2	0.8381E−2	0.8372E−2	0.8395E−2	0.8384E−2
0.010	10	0.7879E−3	0.7856E−3	0.7856E−3	0.7859E−3	0.7858E−3
0.001	18	0.2571E−4	0.2569E−4	0.2569E−4	0.2569E−4	0.2569E−4
$p = 10$						
0.500	2	0.1972E0	0.2018E0	0.2021E0	0.2000E0	0.2000E0
0.200	4	0.5438E−1	0.5348E−1	0.5345E−1	0.5468E−1	0.5384E−1
0.100	6	0.2224E−1	0.2178E−1	0.2174E−1	0.2210E−1	0.2182E−1
0.050	6	0.7667E−2	0.7609E−2	0.7600E−2	0.7628E−2	0.7615E−2
0.010	10	0.7219E−3	0.7198E−3	0.7198E−3	0.7203E−3	0.7201E−3
0.001	18	0.2351E−4	0.2349E−4	0.2349E−4	0.2349E−4	0.2349E−4

Table 2
Comparison of frequency parameter $\overline{\omega} = \omega h\sqrt{\rho_c/E_c}$ vs thickness ratio h/R, vibration modes m and exponent p. Shell data: $b/R = 5$, FGM Al/Al_2O_3.

h/R	m	Ref. Matsunaga (2009)	*LM4*	*ED4*	FSDT	CLT
$p = 1$						
0.500	2	0.8324E−1	0.8808E−1	0.8808E−1	0.8835E−1	0.8824E−1
0.200	4	0.3046E−1	0.2923E−1	0.2923E−1	0.2972E−1	0.2927E−1
0.100	6	0.9585E−2	0.9436E−2	0.9436E−2	0.9482E−2	0.9458E−2
0.050	6	0.3739E−2	0.3726E−2	0.3726E−2	0.3732E−2	0.3731E−2
0.010	10	0.3783E−3	0.3778E−3	0.3778E−3	0.3779E−3	0.3779E−3
0.001	18	0.1201E−4	0.1201E−4	0.1200E−4	0.1200E−4	0.1200E−4
$p = 4$						
0.500	2	0.6737E−1	0.7289E−1	0.7289E−1	0.7322E−1	0.7311E−1
0.200	4	0.2614E−1	0.2481E−1	0.2481E−1	0.2533E−1	0.2488E−1
0.100	6	0.8072E−2	0.7771E−2	0.7910E−2	0.7953E−2	0.7928E−2
0.050	6	0.3075E−2	0.3061E−2	0.3061E−2	0.3066E−2	0.3065E−2
0.010	10	0.3114E−3	0.3108E−3	0.3108E−3	0.3109E−3	0.3109E−3
0.001	18	0.1004E−4	0.1004E−4	0.1004E−4	0.1004E−4	0.1004E−4
$p = 10$						
0.500	2	0.5975E−1	0.6373E−1	0.6372E−1	0.6404E−1	0.6390E−1
0.200	4	0.2325E−1	0.2345E−1	0.2345E−1	0.2411E−1	0.2358E−1
0.100	6	0.7449E−2	0.7453E−2	0.7307E−2	0.7362E−2	0.7332E−2
0.050	6	0.2766E−2	0.2752E−2	0.2751E−2	0.2757E−2	0.2756E−2
0.010	10	0.2809E−3	0.2804E−3	0.2804E−3	0.2805E−3	0.2805E−3
0.001	18	0.9247E−4	0.9241E−4	0.9241E−4	0.9241E−4	0.9241E−4

consist of $[3 \times 3]$ arrays that represent the basic items from which the stiffness matrix of the whole structure can be computed. Detailed derivation procedure is given in the previous works (Carrera, 1999a,b).

For a laminate with N_l layers, the PVD (Eq. (5)) for pure mechanical analysis, neglecting any body forces and considering only applied mechanical loads, is formulated as:

$$\sum_{k=1}^{N_l} \int_{\Omega_k} \int_{A_k} \{\delta\boldsymbol{\epsilon}_{pG}^{k\,T}\boldsymbol{\sigma}_{pC}^{k} + \delta\boldsymbol{\epsilon}_{nG}^{k\,T}\boldsymbol{\sigma}_{nC}^{k}\}\mathrm{d}\Omega_k\mathrm{d}z = \sum_{k=1}^{N_L}\delta L_e^k - \sum_{k=1}^{N_L}\delta L_{in}^k \quad (30)$$

where the integration domains Ω_k and A_k indicate respectively the reference plane of the lamina and its thickness.

Similarly, the RMVT (Eq. (7)) for a laminate becomes:

$$\sum_{k=1}^{N_l} \int_{\Omega_k} \int_{A_k} \{\delta\boldsymbol{\epsilon}_{pG}^{T}\boldsymbol{\sigma}_{pC} + \delta\boldsymbol{\epsilon}_{nG}^{T}\boldsymbol{\sigma}_{n\mathrm{M}} + \delta\boldsymbol{\sigma}_{n\mathrm{M}}^{T}(\boldsymbol{\epsilon}_{nG} - \boldsymbol{\epsilon}_{nC})\}\mathrm{d}\Omega_k\mathrm{d}z = \sum_{k=1}^{N_L}\delta L_e^k - \sum_{k=1}^{N_L}\delta L_{in}^k \quad (31)$$

The steps to obtain the consistent governing equations are: − choice of the opportune variational statement (PVD or RMVT); − substitutions of the consistent constitutive equations; − use of the geometrical relations; − introduction of CUF for the two-dimensional approximation.

In order to obtain a strong form of differential equations on the domain Ω_k, as well as the correspondence boundary conditions on edge Γ_k, the integration by parts is required. Further details on this integration procedure are reported in Carrera et al. (2008). The governing equations on the domain Ω_k, in the PVD case, are:

$$\delta\boldsymbol{u}_s^{k\,T}: \boldsymbol{K}_{uu}^{k\tau sr}\boldsymbol{u}_\tau^k = \boldsymbol{P}_{us}^k - \boldsymbol{M}_{uu}^{k\tau sr}\ddot{\boldsymbol{u}}_\tau^k \quad (32)$$

Boundary conditions of are:

$$\boldsymbol{\Pi}_{uu}^{k\tau sr}\boldsymbol{u}_\tau^k = \boldsymbol{\Pi}_{uu}^{k\tau sr}\overline{\boldsymbol{u}}_\tau^k \quad (33)$$

In Eq. (32), $\boldsymbol{P}_{u\tau}^k$ is the external mechanical load and the fundamental nucleus $\boldsymbol{K}_{uu}^{k\tau sr}$ has to be assembled through the depicted indexes: the internal loop is on index r; τ and s consider the order of

Table 3
Comparison of frequency parameter $\overline{\omega} = \omega h\sqrt{\rho_c/E_c}$ vs thickness ratio h/R, vibration modes m and exponent p. Shell data: $b/R = 10$, FGM Al/Al_2O_3.

h/R	m	Ref. Matsunaga (2009)	*LM4*	*ED4*	FSDT	CLT
$p = 1$						
0.500	2	0.2695E−1	0.2820E−1	0.2820E−1	0.2824E−1	0.2823E−1
0.200	4	0.1038E−1	0.1063E−1	0.1063E−1	0.1064E−1	0.1064E−1
0.100	6	0.5164E−2	0.5230E−2	0.5230E−2	0.5231E−2	0.5231E−2
0.050	6	0.1831E−2	0.1808E−2	0.1808E−2	0.1810E−2	0.1809E−2
0.010	10	0.1897E−3	0.1896E−3	0.1895E−3	0.1896E−3	0.1896E−3
0.001	18	0.5994E−5	0.5992E−5	0.5992E−5	0.5992E−5	0.5992E−5
$p = 4$						
0.500	2	0.2190E−1	0.2345E−1	0.2345E−1	0.2350E−1	0.2349E−1
0.200	4	0.8399E−1	0.8694E−1	0.8694E−1	0.8699E−1	0.8698E−1
0.100	6	0.2391E−2	0.4250E−2	0.4250E−2	0.4251E−2	0.4251E−2
0.050	6	0.1568E−2	0.1543E−2	0.1543E−2	0.1545E−2	0.1543E−2
0.010	10	0.1547E−3	0.1545E−3	0.1545E−3	0.1545E−3	0.1545E−3
0.001	18	0.4963E−5	0.4961E−5	0.4961E−5	0.4961E−5	0.4961E−5
$p = 10$						
0.500	2	0.1947E−1	0.2037E−1	0.2037E−1	0.2042E−1	0.2040E−1
0.200	4	0.7411E−1	0.7601E−1	0.7601E−1	0.7604E−1	0.7604E−1
0.100	6	0.3677E−2	0.3728E−2	0.3728E−2	0.3729E−2	0.3729E−2
0.050	6	0.1478E−2	0.1457E−2	0.1457E−2	0.1460E−2	0.1458E−2
0.010	10	0.1378E−3	0.1377E−3	0.1377E−3	0.1377E−3	0.1377E−3
0.001	18	0.4515E−5	0.4512E−5	0.4512E−5	0.4512E−5	0.4512E−5

Table 4
Comparison of frequency parameter $\overline{\omega} = \omega h\sqrt{\rho_c/E_c}$ vs thickness ratio h/R, vibration modes m and exponent p. Shell data: $b/R = 20$, FGM Al/Al_2O_3.

h/R	m	Ref. Matsunaga (2009)	*LM*4	*ED*4	FSDT	CLT
$p = 1$						
0.500	2	0.7990E−2	0.7732E−2	0.7731E−2	0.7738E−2	0.7737E−2
0.200	4	0.2875E−2	0.2905E−2	0.2905E−2	0.2906E−2	0.2906E−2
0.100	6	0.1413E−2	0.1426E−2	0.1426E−2	0.1427E−2	0.1427E−2
0.050	6	0.7032E−3	0.7076E−3	0.7076E−3	0.7076E−3	0.7076E−3
0.010	10	0.7733E−4	0.7714E−4	0.7714E−4	0.7716E−4	0.7716E−4
0.001	18	0.2783E−5	0.2782E−5	0.2782E−5	0.2782E−5	0.2782E−5
$p = 4$						
0.500	2	0.6562E−2	0.6445E−2	0.6444E−2	0.6451E−2	0.6450E−2
0.200	4	0.2331E−2	0.2377E−2	0.2377E−2	0.2377E−2	0.2377E−2
0.100	6	0.1143E−2	0.1160E−2	0.1160E−2	0.1160E−2	0.1160E−2
0.050	6	0.5684E−3	0.5735E−3	0.5735E−3	0.5735E−3	0.5735E−3
0.010	10	0.6564E−4	0.6543E−4	0.6543E−4	0.6544E−4	0.6544E−4
0.001	18	0.2319E−5	0.2318E−5	0.2317E−5	0.2318E−5	0.2318E−5
$p = 10$						
0.500	2	0.5913E−2	0.5584E−2	0.5583E−2	0.5590E−2	0.5589E−2
0.200	4	0.2064E−2	0.2076E−2	0.2076E−2	0.2076E−2	0.2076E−2
0.100	6	0.1008E−2	0.1017E−2	0.1017E−2	0.1017E−2	0.1017E−2
0.050	6	0.5007E−3	0.5038E−3	0.5038E−3	0.5039E−3	0.5039E−3
0.010	10	0.6144E−4	0.6126E−4	0.6126E−4	0.6128E−4	0.6127E−4
0.001	18	0.2125E−5	0.2124E−5	0.2123E−5	0.2124E−5	0.2124E−5

expansion in z for the displacements; superscript k indicates the assembling on the number of layers. $\ddot{\boldsymbol{u}}_\tau^k$ denotes the second derivative with respect to the time of the displacement components and matrix $\boldsymbol{M}_{uu}^{k\tau sr}$ represents the fundamental nucleus for the inertial array:

$$\boldsymbol{M}^{k\tau sr} = \int_{A_k} \boldsymbol{I}\rho_r^k F_\tau F_s F_r \mathrm{d}z, \tag{34}$$

the fundamental nucleus $\boldsymbol{K}_{uu}^{k\tau sr}$ for the stiffness matrix and the fundamental nucleus $\boldsymbol{\Pi}_{uu}^{k\tau sr}$ for the boundary conditions are:

$$\begin{aligned}\boldsymbol{K}_{uu}^{k\tau sr} = \int_{A_k} [&(-\boldsymbol{D}_p^k + \boldsymbol{A}_p^k)^T (F_r \boldsymbol{Q}_{ppr}^k (\boldsymbol{D}_p^k + \boldsymbol{A}_p^k) + F_r \boldsymbol{Q}_{pnr}^k (\boldsymbol{D}_{np}^k + \boldsymbol{D}_{nz}^k - \boldsymbol{A}_n^k)) \\ &+ (-\boldsymbol{D}_{np}^k + \boldsymbol{D}_{nz}^k - \boldsymbol{A}_n^k)^T (F_r \boldsymbol{Q}_{npr}^k (\boldsymbol{D}_p^k + \boldsymbol{A}_p^k) \\ &+ F_r \boldsymbol{Q}_{nnr}^k (\boldsymbol{D}_{np}^k + \boldsymbol{D}_{nz}^k - \boldsymbol{A}_n^k))] F_s F_\tau H_\alpha^k H_\beta^k \mathrm{d}z,\end{aligned} \tag{35}$$

$$\begin{aligned}\Pi_{uu}^{k\tau sr} = \int_{A_k} [&\boldsymbol{I}_p^{kT} (F_r \boldsymbol{Q}_{ppr}^k (\boldsymbol{D}_p^k + \boldsymbol{A}_p^k) + F_r \boldsymbol{Q}_{pnr}^k (\boldsymbol{D}_{np}^k + \boldsymbol{D}_{nz}^k - \boldsymbol{A}_n^k)) \\ &+ \boldsymbol{I}_{np}^{kT} (F_r \boldsymbol{Q}_{npr}^k (\boldsymbol{D}_p^k + \boldsymbol{A}_p^k) + F_r \boldsymbol{Q}_{nnr}^k (\boldsymbol{D}_{np}^k + \boldsymbol{D}_{nz}^k - \boldsymbol{A}_n^k))] \\ &\times F_s F_\tau H_\alpha^k H_\beta^k \mathrm{d}z.\end{aligned} \tag{36}$$

$\boldsymbol{I}_p^k$ and $\boldsymbol{I}_{np}^k$ are identity matrices to perform the integration by parts.

$$\boldsymbol{I} = \begin{bmatrix} 1 & 0 & 0 \\ 0 & 1 & 0 \\ 0 & 0 & 1 \end{bmatrix}, \quad \boldsymbol{I}_p^k = \begin{bmatrix} \frac{1}{H_\alpha^k} & 0 & 0 \\ 0 & \frac{1}{H_\beta^k} & 0 \\ \frac{1}{H_\beta^k} & \frac{1}{H_\alpha^k} & 0 \end{bmatrix}, \quad \boldsymbol{I}_{np}^k = \begin{bmatrix} 0 & 0 & \frac{1}{H_\alpha^k} \\ 0 & 0 & \frac{1}{H_\beta^k} \\ 0 & 0 & 0 \end{bmatrix}. \tag{37}$$

Further details about fundamental nuclei in Eqs. (34)–(36) can be found in Carrera et al. (2008).

The governing equations in the RMVT case are:

$$\begin{aligned}\delta \boldsymbol{u}_s^k &: \boldsymbol{K}_{uu}^{k\tau sr} \boldsymbol{u}_\tau^k + \boldsymbol{K}_{u\sigma}^{k\tau sr} \sigma_{n\tau}^k = \boldsymbol{P}_{us}^k - \boldsymbol{M}^{k\tau sr} \ddot{\boldsymbol{u}}_\tau^k \\ \delta \sigma_{ns}^k &: \boldsymbol{K}_{\sigma u}^{k\tau sr} \boldsymbol{u}_\tau^k + \boldsymbol{K}_{\sigma\sigma}^{k\tau sr} \sigma_{n\tau}^k = 0\end{aligned} \tag{38}$$

Table 5
Comparison of frequency parameter $\overline{\omega} = \omega h\sqrt{\rho_c/E_c}$ vs thickness ratio h/R, vibration modes m and exponent p. Shell data: $b/R = 2$, FGM Al/Al_2O_3.

p	h/R	m	Ref. Matsunaga (2009)	Natural frequency					
				*LM*4	*ED*4	*LD*3	*ED*2	CLT	FSDT
1	0.500	2	0.2720E0	0.2768E0	0.2765E0	0.2768E0	0.2771E0	0.2811E0	0.2778E0
	0.200	4	0.7218E−1	0.7113E−1	0.7117E−1	0.7113E−1	0.7119E−1	0.7206E−1	0.7137E−1
	0.100	6	0.2821E−1	0.2766E−1	0.2771E−1	0.2766E−1	0.2768E−1	0.2792E−1	0.2770E−1
	0.050	6	0.1020E−1	0.1013E−1	0.1013E−1	0.1013E−1	0.1013E−1	0.1015E−1	0.1014E−1
	0.010	10	0.9454E−3	0.9434E−3	0.9446E−3	0.9434E−3	0.9434E−3	0.9438E−3	0.9436E−3
	0.001	18	0.3068E−4	0.3090E−4	0.3090E−4	0.3090E−4	0.3090E−4	0.3090E−4	0.3090E−4
4	0.500	2	0.2209E0	0.2261E0	0.2258E0	0.2262E0	0.2267E0	0.2313E0	0.2280E0
	0.200	4	0.5995E−1	0.5879E−1	0.5884E−1	0.5880E−1	0.5893E−1	0.5980E−1	0.5912E−1
	0.100	6	0.2391E−1	0.2330E−1	0.2334E−1	0.2330E−1	0.2335E−1	0.2359E−1	0.2336E−1
	0.050	6	0.8449E−2	0.8372E−2	0.8381E−2	0.8372E−2	0.8375E−2	0.8395E−2	0.8384E−2
	0.010	10	0.7879E−3	0.7856E−3	0.7856E−3	0.7856E−3	0.7856E−3	0.7860E−3	0.7858E−3
	0.001	18	0.2571E−4	0.2569E−4	0.2569E−4	0.2569E−4	0.2569E−4	0.2569E−4	0.2569E−4
10	0.500	2	0.1972E0	0.2021E0	0.2018E0	0.2021E0	0.2030E0	0.2000E0	0.2000E0
	0.200	4	0.5438E−1	0.5344E−1	0.5348E−1	0.5345E−1	0.5367E−1	0.5469E−1	0.5384E−1
	0.100	6	0.2224E−1	0.2174E−1	0.2178E−1	0.2174E−1	0.2181E−1	0.2210E−1	0.2182E−1
	0.050	6	0.7667E−2	0.7601E−2	0.7609E−2	0.7601E−2	0.7604E−2	0.7628E−2	0.7615E−2
	0.010	10	0.7219E−3	0.7198E−3	0.7198E−3	0.7198E−3	0.7199E−3	0.7203E−3	0.7201E−3
	0.001	18	0.2351E−4	0.2349E−4	0.2349E−4	0.2349E−4	0.2349E−4	0.2349E−4	0.2349E−4

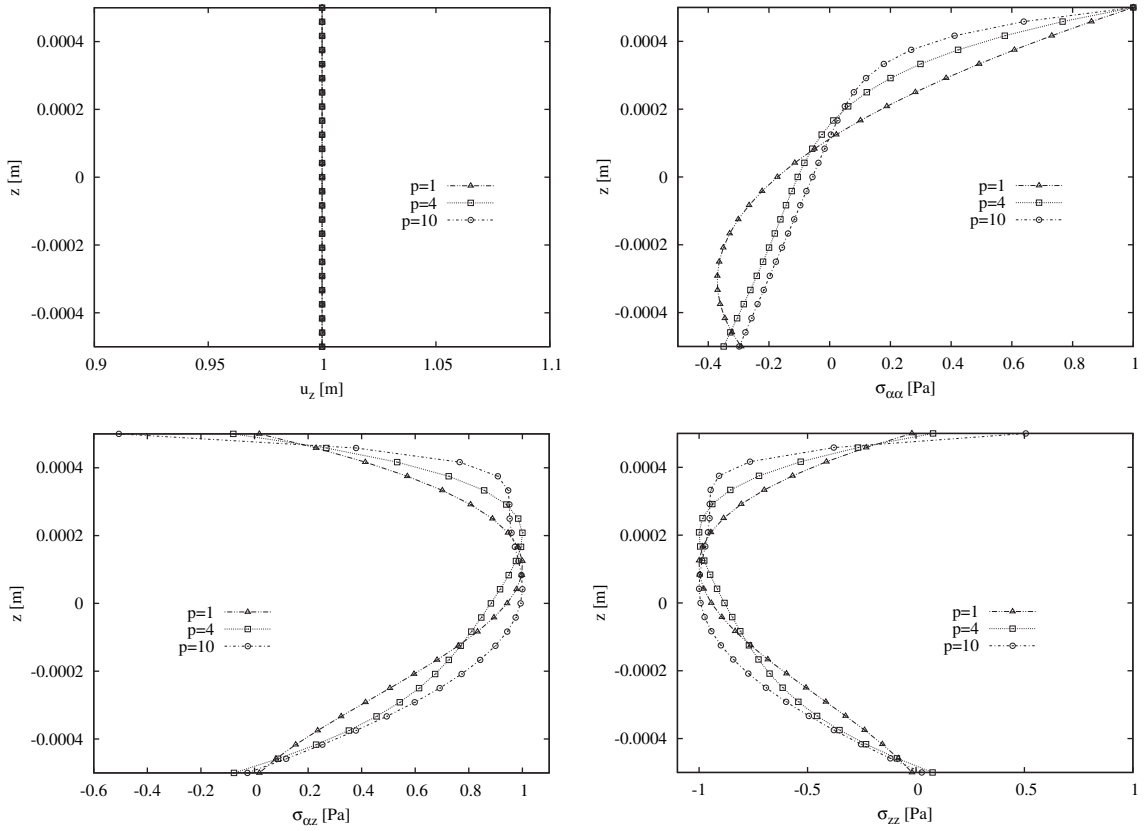

Fig. 2. Through the thickness distributions of stresses and displacements far various p values. Data $h = R = 0.001$ $b = R = 10$, ED4 results.

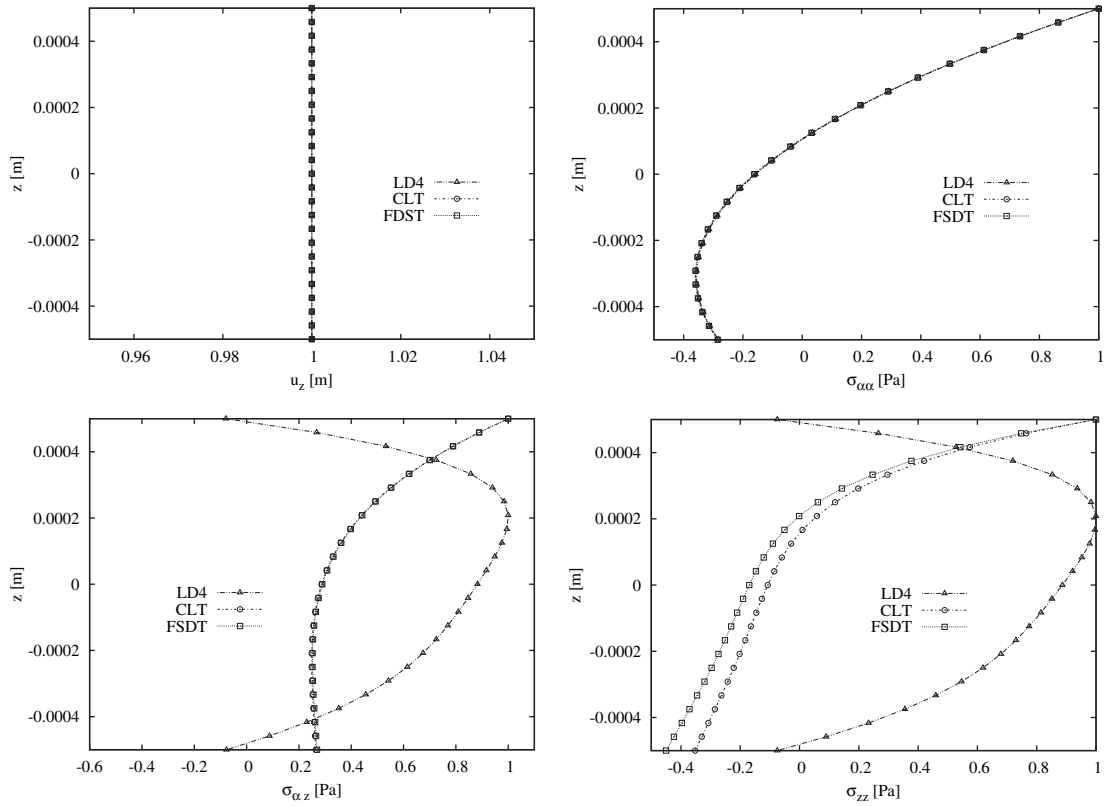

Fig. 3. Through the thickness distributions of stresses and displacements far various p values. Data $b = R = 2$ and $h = R = 0.001$.

four fundamental nuclei relative to stiffness array are obtained. These are completely different from those obtained in the PVD case while the inertial array does not change.

Corresponding boundary conditions of Neumann type are:

$$\boldsymbol{\Pi}^{k\tau sr}_{uu}\boldsymbol{u}^k_\tau + \boldsymbol{\Pi}^{k\tau sr}_{u\sigma}\boldsymbol{\sigma}^k_{n\tau} = \boldsymbol{\Pi}^{k\tau sr}_{uu}\overline{\boldsymbol{u}}^k_\tau + \boldsymbol{\Pi}^{k\tau sr}_{u\sigma}\overline{\boldsymbol{\sigma}}^k_{n\tau} \tag{39}$$

The fundamental nuclei can be obtained:

$$\boldsymbol{K}^{k\tau sr}_{uu} = \int_{A_k}\left[(-\boldsymbol{D}^k_p+\boldsymbol{A}^k_p)^T\left(F_r\widehat{\boldsymbol{Q}}^k_{ppr}(\boldsymbol{D}^k_p+\boldsymbol{A}^k_p)\right)\right]F_sF_\tau H^k_\alpha H^k_\beta \mathrm{d}z, \tag{40}$$

$$\boldsymbol{K}^{k\tau sr}_{u\sigma} = \int_{A_k}\left[(-\boldsymbol{D}^k_p+\boldsymbol{A}^k_p)^T\left(F_r\widehat{\boldsymbol{Q}}^k_{pnr}\right)+(-\boldsymbol{D}^k_{np}+\boldsymbol{D}^k_{nz}-\boldsymbol{A}^k_n)^T\right] \times F_sF_\tau H^k_\alpha H^k_\beta \mathrm{d}z, \tag{41}$$

$$\boldsymbol{K}^{k\tau sr}_{\sigma u} = \int_{A_k}\left[(\boldsymbol{D}^k_{np}+\boldsymbol{D}^k_{nz}-\boldsymbol{A}^k_n)-\left(F_r\widehat{\boldsymbol{Q}}^k_{npr}\right)(\boldsymbol{D}^k_p+\boldsymbol{A}^k_p)\right] \times F_sF_\tau H^k_\alpha H^k_\beta \mathrm{d}z, \tag{42}$$

$$\boldsymbol{K}^{k\tau sr}_{\sigma\sigma} = \int_{A_k}\left[-F_r\widehat{\boldsymbol{Q}}^k_{nnr}\right]F_sF_\tau H^k_\alpha H^k_\beta \mathrm{d}z, \tag{43}$$

The nuclei for boundary conditions on edge Γ_k are:

$$\boldsymbol{\Pi}^{k\tau sr}_{uu} = \int_{A_k}\left[\boldsymbol{I}^{kT}_p F_r\widehat{\boldsymbol{Q}}^k_{ppr}(\boldsymbol{D}^k_p+\boldsymbol{A}^k_p)\right]F_sF_\tau H^k_\alpha H^k_\beta \mathrm{d}z, \tag{44}$$

$$\boldsymbol{\Pi}^{k\tau sr}_{u\sigma} = \int_{A_k}\left[\boldsymbol{I}^{kT}_p F_r\widehat{\boldsymbol{Q}}^k_{pnr}+\boldsymbol{I}^{kT}_{np}\right]F_sF_\tau H^k_\alpha H^k_\beta \mathrm{d}z. \tag{45}$$

6. Closed-form solution for free-vibration problem

For the derived boundary value problem, for particular geometry, material symmetry and boundary conditions, an analytical solution can be derived. For simply supported shells, a Navier-type closed-form solution may be found with the following harmonic assumptions for the field variables:

$$\begin{aligned}
\left(u^k_{\alpha_\tau},\sigma^k_{\alpha z_\tau}\right) &= \sum_{m,n}\left(\widehat{U}^k_{\alpha_\tau},\widehat{S}^k_{\alpha z_\tau}\right)\cos\frac{m\pi\alpha_k}{a_k}\sin\frac{n\pi\beta_k}{b_k}e^{i\omega_{mn}t}, \quad k=1,N_l,\\
\left(u^k_{\beta_\tau},\sigma^k_{\beta z_\tau}\right) &= \sum_{m,n}\left(\widehat{U}^k_{\beta_\tau},\widehat{S}^k_{\beta z_\tau}\right)\sin\frac{m\pi\alpha_k}{a_k}\cos\frac{n\pi\beta_k}{b_k}e^{i\omega_{mn}t}, \quad \tau=t,b,r,\\
\left(u^k_{z_\tau},\sigma^k_{zz_\tau}\right) &= \sum_{m,n}\left(\widehat{U}^k_{z_\tau},\widehat{S}^k_{zz_\tau}\right)\sin\frac{m\pi\alpha_k}{a_k}\sin\frac{n\pi\beta_k}{b_k}e^{i\omega_{mn}t}, \quad r=2,N,
\end{aligned} \tag{46}$$

where a_k and b_k are the lengths of the shell along the two curvilinear coordinates α and β. m and n represent the number of half-waves in α and β direction, respectively. These numbers characterize the vibration mode associated to the circular frequency ω_{mn}. $i=\sqrt{-1}$ is the imaginary unit and t the time. The quantities with $\widehat{\cdot}$ indicate the amplitudes. These assumptions correspond to the simply supported boundary conditions. Upon substitution of Eq. (46), the governing equations on Ω^k assume the form of a linear system of algebraic equations in the domain, while the boundary conditions are exactly fulfilled.

Only the free-vibration analysis is addressed in this article. Therefore, the external mechanical loading is set to zero and the linear system of algebraic equations is:

$$\boldsymbol{K}^*\widehat{\boldsymbol{U}} = \omega^2_{mn}\boldsymbol{M}\widehat{\boldsymbol{U}}, \tag{47}$$

where $\boldsymbol{K}^*$ is the equivalent stiffness matrix obtained by means of static condensation (for further details see Carrera, 1998b, 2000), $\boldsymbol{M}$ is the inertial matrix and $\widehat{\boldsymbol{U}}$ is the vector of unknown variables. By defining $\lambda_{mn}=\omega^2_{mn}$, the solution of the associated eigenvalue problem becomes:

$$||\boldsymbol{K}^*-\lambda_{mn}\widehat{\boldsymbol{M}}|| = 0. \tag{48}$$

The eigenvectors $\widehat{\boldsymbol{U}}$ associated to the eigenvalues λ_{mn} (or to circular frequencies ω_{mn}) define the vibration modes of the structure in terms of primary variables. Once the wave numbers (m,n) have been defined in the in-plane directions, the number of obtained frequencies becomes equal to the degrees of freedom of the employed two-dimensional model. It is possible to obtain the related eigenvector, in terms of primary variables, for each value of frequency, in order to plot the modes in the thickness direction.

7. Numerical results

The developed shell theories have first been applied to compare the results with the available reference solutions (Matsunaga, 2009) in which higher order ESL type shell theories were developed ($N=1,2,3,4$). The adopted grading law distribution is that of Zenkour (2006); Young's Modulus, shear modulus and density, vary

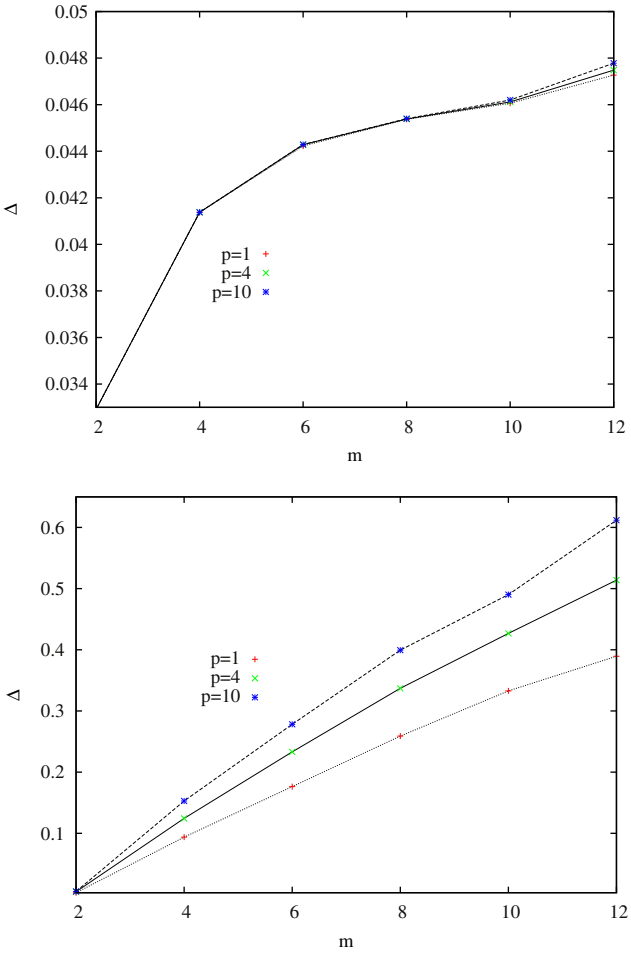

Fig. 4. Errors of CLT vs ED4 comparison through the errors in fundamental frequency for wave number m increased. Thin (right) and thick (left) shells compared for several p value.

Table 6
Comparison of frequency parameter $\overline{\omega} = \omega h\sqrt{\rho_c/E_c}$ vs thickness ratio h/R, vibration modes m and exponent p for multilayered shell. Data: $b/R = 20$, $m = 2$.

p	*LM4*	*LD4*	*ED4*	*LD3*	*ED2*	FSDT	CLT
$h/R = 0.5$							
1	0.2905E0	0.2905E0	0.2905E0	0.2906E0	0.2908E0	0.2764E0	0.2768E0
4	0.2521E0	0.2521E0	0.2521E0	0.2520E0	0.2523E0	0.2393E0	0.2397E0
10	0.2368E0	0.2368E0	0.2368E0	0.2368E0	0.2369E0	0.2237E0	0.2243E0
$h/R = 0.001$							
1	0.5165E−3	0.5165E−3	0.5165E−3	0.5165E−3	0.5165E−3	0.4995E−3	0.4995E−3
4	0.4407E−3	0.4407E−3	0.4408E−3	0.4407E−3	0.4408E−3	0.4263E−3	0.4263E−3
10	0.4056E−3	0.4056E−3	0.4058E−3	0.4056E−3	0.4058E−3	0.3924E−3	0.3924E−3

continuously through the thickness, accordingly to the change in volume fractions of the materials, which takes place according to the law:

$$\wp = \wp_m + (\wp_c - \wp_m)\left(\frac{1}{2} + \frac{z}{h}\right)^p \tag{49}$$

where $\wp_m$ is the property of the metallic phase, $\wp_c$ is the property of the ceramic phase, h is the global thickness and z is the variation in the thickness coordinate, which varies between $-h/2$ and $h/2$, and p is the power law exponent.

In order to validate the accuracy of the proposed theories for free-vibration analysis of FGM shells, various shell configuration have been examined by changing the length (a,b), radius (R), thickness (h), vibration modes (m) and grading law exponent (p) in the FGM layer of the cylindrical shell.

For the sake of conciseness, only the results related to significant shell theories have been reported in the following analysis. In most classical cases CLT and FSDT results are compared to the higher order ESLM theory (*ED4*) and to layer-wise mixed analysis with fourth-order expansion in each layer. The last shell theory has been proved in previous works by the authors Carrera (1998a), Carrera et al. (2008), to lead to a quasi three-digressional description of the statics and dynamics of layered structures. Tables 1–4 compare the present analysis with those in Matsunaga (2009) for a FGM circular cylindrical, simply supported shell made of aluminium ($E_m = 70$ GPa, $\rho_m = 2702$ kg/m^3, $\nu = 0.3$) at the bottom and alumina (Al_2O_3) ($E_c = 380$ GPa, $\rho_m = 3800$ kg/m^3, $\nu = 0.3$) at the top. The geometry of the shell varies according to the b/R and h/R ratio, fixing $R = R_\alpha = R_\beta = 1[m]$ and $a = \pi$, where a is the length along the α coordinate and b is the length along the β coordinate. The 4 tables are related to the evaluation of frequency parameter $\overline{\omega}$ for the following values of length-to-radius ratio $b/R = 2$, 5, 10, 20, respectively. Various values of the thickness-to-radius h/R

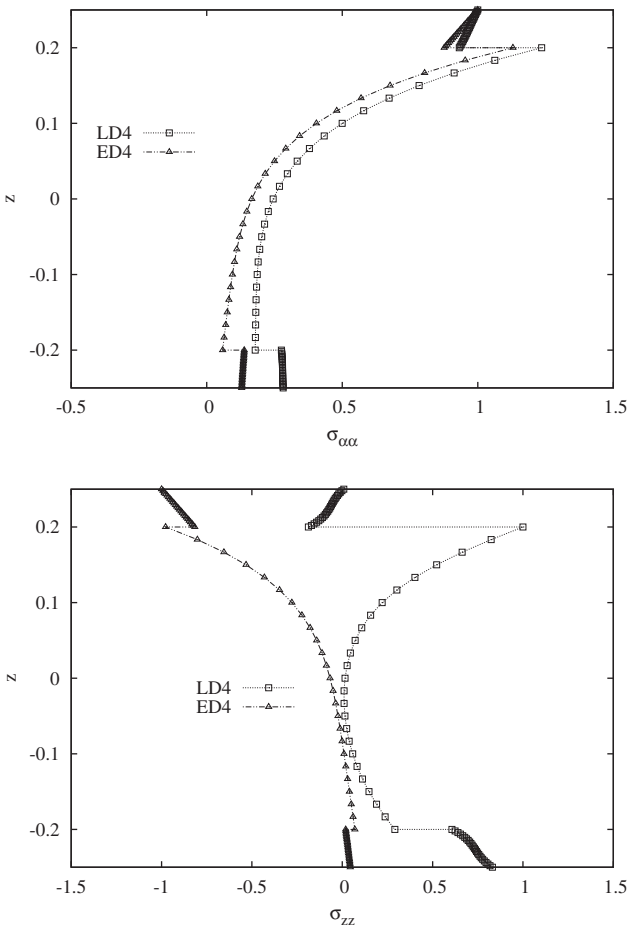

Fig. 5. Through the thickness distributions of stresses for p = 4 for a three layered shell. Comparison between LD4 and ED4 results. Data $b = R = 2$, $m = 2$ and $h = R = 0.5$.

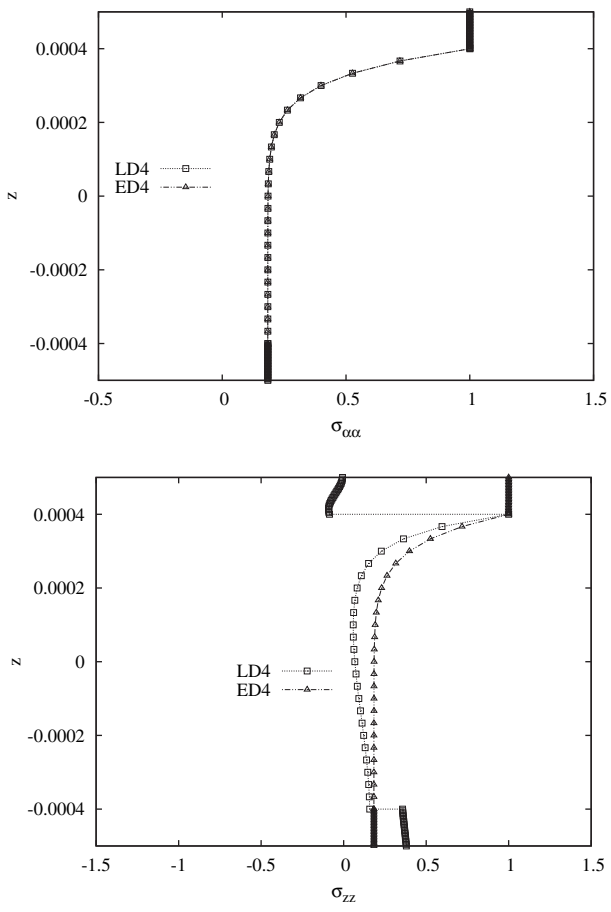

Fig. 6. Through the thickness distributions of stresses for p = 10 for a three layered shell. Comparison between LD4 and ED4 results. Data $b = R = 2$, $m = 2$ and $h = R = 0.001$.

parameter, the wave number m of the vibration modes along the α direction (n value is fixed to 1) and the grading law exponent are considered in each table. For thin single-layered shells, the highest forth-order *ED*4 theory provides almost the same results of the reference solution (Matsunaga, 2009); classic theories are not able to describe the correct dynamic behavior, especially for a thick shell geometry. Such a discrepancy is almost negligible in thin shell cases. The use of refined theories appears mandatory in order to obtain accurate results; this is confirmed in Table 5 where a comparison with additional classical and advanced theories is given. Since three-dimensional elasticity solutions are not available for the considered shell problems, the authors advice is to consider the present *LM*4 analysis as a quasi-3D solution, i.e. as a reference solution.

Since frequency parameters are global characteristic of a shell dynamic response, a better exploitation of the response of various shell theories could be obtained by considering the distribution of vibration modes in the thickness shell directions. This has been done in Figs. 2 and 3.The displacements and stresses are compared in Fig. 2 which accounts for three different values of grading parameter p. The *ED*4 results show that the differences in the response of the considered p values are affected to a greater extent by the values of the thickness coordinate z. Layer-wise results with $N = 4$ (*LD*4) are compared in Fig. 3 with classical CLT and first-order SDT (FSDT). The differences increase in the case of the transverse shear and normal stress evaluation. It appears clear that classical theories even though, such as CLT and FSDT, could lead to acceptable results in the evaluation of free-vibration parameters, they could fail completely to describe stress/displacement fields in the thickness direction of the considered vibration modes. In other words CLT and FSD are not adequate to detect failures of FGM shells due to vibrations.

The differences between the CLT and *ED*4 results $\Delta = (ED4 - \mathrm{CLT})/ED4$ are given in Fig. 4. It has been confirmed that the errors of classical theories increase by vibration mode increasing. It has also been confirmed that *ED*4 provides good results according to the reference solution, for single-layer shells. A multilayered shell made up of two isotropic skins (Al at the top and Al_2O_3 at the bottom) embedding a FGM core is presented. Fundamental free frequency values are reported in Table 6, where several theories are compared. A thick and a thin shell are analyzed.

Table 6 confirms the convenience of referring to refined models, especially in the case of thick shells. In addition, Figs. 5 and 6 show the limitations of ESL type models in tracing through-the-thickness distributions of various stress variables. The use of layer-wise models, such as *LD*4, appears mandatory in these cases.

8. Conclusions

A free-vibration problem of multilayered shells embedding FGM layers has been considered in this work by referring to variable kinematic shell theories developed in the framework of the Carrera Unified Formulation. Attention has been restricted to orthotropic, simply supported, shells. Classical theories are compared to higher order ones as well as to layer-wise kinematic and mixed shell formulations based on the Reissner Mixed Variational Theorem. The conducted numerical analysis has shown that the accuracy of various theories depends to a great extent on various geometrical parameters as well as on the dynamic modes. The proposed variable kinematic model therefore appears to be able to obtain exact values and to establish the accuracy of classical shell theories, especially for multilayered shells.

References

Birman, V., Bird, L.W., 2007. Modeling and analysis of functionally graded materials and structures. Applied Mechanics Reviews 60, 195–216.

Brischetto, S., Carrera, E., 2008. Advanced mixed theories for bending analysis of functionally graded plates. Computers and Structures, in press, available on line on May 2008.

Carrera, E., 1995. A class of two dimensional theories for multilayered plates analysis. Atti Accademia delle Scienze di Torino. Memorie Scienze Fisiche 19–20, 49–87.

Carrera, E., 1998a. Evaluation of layer-wise mixed theories for laminated plates analysis. AIAA Journal 26, 830–839.

Carrera, E., 1998b. Layer-wise mixed models for accurate vibration analysis of multilayered plates. Journal of Applied Mechanics 65, 820–828.

Carrera, E., 1999a. Multilayered shell theories accounting for layerwise mixed description – part I, II – governing equations and numerical evluations. AIAA Journal 37, 1107–1124.

Carrera, E., 1999b. A study of transverse normal stress effect on vibration of multylayered plates and shells. Journal of Sound and Vibrations 225 (5), 803–829.

Carrera, E., 2000. An assessment of mixed and classical theories on global and local response of multilayered, orthotropic plates. Computers and Structures 50, 183–198.

Carrera, E., 2001. Developments, ideas, and evaluations based upon Reissner's Mixed Variational Theorem in the modeling of multilayered plates and shells. Applied Mechanics Reviews 54, 301–329.

Carrera, E., 2002. Theories and finite elements for multilayered anisotropic, composite plates and shells. Archives of Computational Methods in Engineering 9, 87–140.

Carrera, E., 2003. Theories and finite elements for multilayered plates and shells: a unified compact formulation with numerical assessments and benchmarks. Archivies of Computational Methods in Engineering 10, 215–296.

Carrera, E., Brischetto, S., Robaldo, A., 2008. Variable kinematic model for the analysis of functionally graded material plates. AIAA Journal 46, 194–203.

Carrera, E., Brischetto, S., 2008a. Analysis of thickness locking in classical, refined and mixed multilayered plate theories. Composite Structures 82, 549–562.

Carrera, E., Brischetto, S., 2008b. Analysis of thickness locking in classical, refined and mixed theories for layered shells. Composite Structures 85, 83–90.

Carrera, E., Brischetto, S., Cinefra, M., Soave, M. Refined and advanced models for multilayered plates and shells embedding functionally graded material layers, in press.

Cauchy, A.L., 1828. Sur l'equilibre et le mouvement d'une plaque solide. Exercises de Matematique 3, 328–355.

Chen, W.Q., Bian, Z.G., Ding, H.J., 2004. Three-dimensional vibration analysis of fluid-filled orthotropic FGM cylindrical shells. International Journal of Mechanical Sciences 46, 159–171.

Cinefra, M., Soave M. Accurate vibration analysis of multilayered plates made of functionally graded materials, in press.

Giunta, G., Belouettar, S., Carrera, E. Analysis of FGM beams by means of classical and advanced theories, in press.

Kashtalyan, M., 2004. Three-dimensional elasticity solution for bending of functionally graded rectangular plates. European Journal of Mechanics A Solids 23, 853–864.

Kirchhoff, G., 1850. Uber das Gleichgewicht und die Bewegung einer elastishen Scheibe. Crelles Journal 40, 51–88.

Kraus, H., 1967. Thin Elastic Shells. John Wiley, New York.

Loy, C.T., Lam, K.Y., Reddy, J.N., 1999. Vibration of functionally graded cylindrical shells. International Journal of Mechanical Sciences 41, 309–324.

Matsunaga, H., 2009. Free vibration and stability of functionally graded circular cylindrical shells according to a 2D higher-order deformation theory. Composite Structure 88, 519–531.

Mindlin, R.D., 1951. Influence of rotatory inertia and shear in flexural motions of isotropic elastic plates. Journal of Applied Mechanics 18, 31–38.

Mori, T., Tanaka, K., 1973. Average stress in matrix and average elastic energy of materials with misfitting inclusions. Acta Metallurgica 21, 571–574.

Poisson, S.D., 1829. Memoire sur l'equilibre et le mouvement des corps elastique. Memory Academic Science 8, 357.

Pradhan, S.C., Loy, C.T., Lam, K.Y., Reddy, J.N., 2000. Vibration characteristics of functionally graded cylindrical shells under various boundary conditions. Applied Acoustics 61, 111–129.

Reddy, J.N., 2004. Mechanics of Laminated Composite Plates, Theory and Analysis. CRC Press, New York.

Reissner, E., 1945. The effect of transverse shear deformation on the bending of elastic plates. Journal of Applied Mechanics 12, 69–76.

Reissner, E., 1984. On a certain mixed variational theory and a proposed application. International Journal for Numerical Methods in Engineering 20, 1366–1368.

Tornabene, F., 2009. Free vibration analysis of functionally graded conical, cylindrical shell and annular plate structures with a four-parameter power-law distribution. Computer Methods in Applied Mechanics and Engineering 198 (37–40), 2911–2935.

Washizu, K., 1968. Variational Methods in Elasticity and Plasticity. Pergamon Press, New York.

Zenkour, A.M., 2006. Generalized shear deformation theory for bending analysis of functionally graded plates. Applied Mathematical Modelling 30, 67–84.